

IFSCC 2025 full paper (IFSCC2025-1607)

Sex-Based Differences Modulate Skin Physiology and Dictate Sensorial Perception of Cosmetic Formulations

Ashley David¹, Sebastian Hendrickx-Rodriguez², Rachele Pia Russo¹, Heiva Le Blay³, Muriel Liboutet⁴, Anne Bouchara⁴, Gustavo S. Luengo³, Anne Potter³, Reinhold H. Dauskardt¹

¹Department of Materials Science and Engineering, Stanford University, Stanford, CA, USA

²Department of Mechanical Engineering, Stanford University, Stanford, CA, USA

³L'Oréal Research and Innovation, Aulnay-sous-Bois, France

⁴L'Oréal Research and Innovation, Chevilly-Larue, France

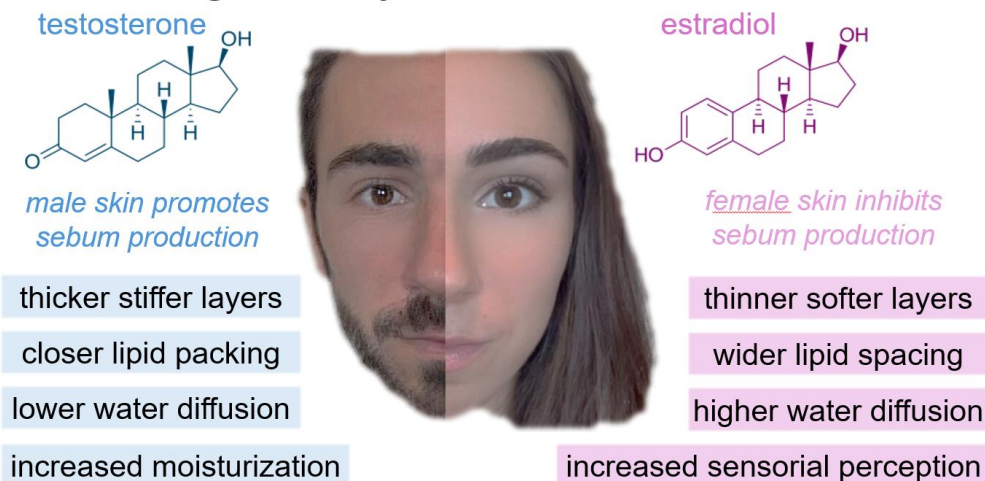
1. Introduction

Sensory neuron activation arises from changes in stratum corneum (SC) biomechanics modulated by topical treatments influences skin sensory perception like the feeling of skin tightness.[1] The effect of key sex-based differences in the structure and composition of human SC and the underlying skin layers (e.g. sebum, pH, corneocyte size, intercellular lipids, epidermal & dermal thickness/stiffness) on such sensorial perception in response to cosmetic formulations are poorly understood (**Fig 1.**). We study these effects with *ex vivo* experimental assays and computational neurological models and reveal new insights in their role in water transport, moisturization, mechanoreceptor activation, and sensory perception following cosmetic treatments in male and female skin.

Ex vivo SC samples from over 20 male and female donors were analyzed using high resolution techniques like synchrotron X-ray diffraction and infrared spectroscopy, to examine SC lateral and lamellar lipid structure, sebum quantity and dehydration rates. Mechanical stress was assessed, tracking stress evolution over 20-40 hours after applying six moisturizing formulations. Computational modeling, incorporating sex-specific skin physiology, explored formulation effects on sensory neuron activation related to skin comfort.

Consumer studies and clinical evaluations further assessed perceived skin feel, sensitivity, and dryness. By understanding how sex-based biochemical, anatomical, and mechanical differences coordinate to shape the distinct sensory experience of each demographic, the

Enhancing Beauty for Male and Female Skin



Study highlights acute biological differences between male and female skin underscoring the importance of sex-specific needs in personalized cosmetic products.

Figure 1. Sex-based differences in stratum corneum (SC) structure and function. Biochemical cues, in particular the hormones testosterone and estradiol, regulate downstream pathways that influence SC architecture. These structural variations impact key SC properties and overall barrier function [2],[3],[4],[5].

objective of our study is to provide the underlying understanding from which we can maximize the efficacy of cosmetic treatments for males and females.

2. Materials and Methods

Skin Processing

SC samples were extracted from full-thickness abdominal skin from male and female Caucasian human between 40-80 years old obtained from the National Disease Research Interchange and stored in a -80°C freezer. SC was isolated from the full-thickness skin by removing subcutaneous tissue, soaking sample in 35°C water for 10 minutes and 60°C water for 1 minute, mechanically separating the dermis from the epidermis, and finally removing the remaining epidermis by placing the sample in a trypsin enzymatic digest solution [0.1% (wt/wt) in 0.05 M, pH 8.3 Tris buffer] at 35°C for 180 minutes. The SC was then rinsed, dried on filter paper, and stored in a ~10-20% RH humidity chamber at ~18-23°C. As the work does not involve human subjects per standard guidelines, ethics approvals were therefore not required.

Ex-vivo Substrate Curvature Technique

Stresses in the SC were measured using thin film mechanics techniques by attaching the SC to a borosilicate glass beam coated with Cr/Au on one side [6],[7]. One end of the substrate was pinned down, while the other end formed a parallel-plate capacitor with a sensor. The samples were dried in a humidity below 5% RH and temperature of ~23°C, inducing SC stresses that deflect the cantilever substrate by an amount measurable by the capacitive

sensor. The cantilever beam deflection, δ , was used to calculate SC film stresses with Stoney's Equation:

$$\sigma_{SC} = \left(\frac{E_{sub}}{1 - \nu_{sub}} \right) \left(\frac{h_{sub}^2}{3h_{SC}L^2} \right) \delta$$

where E_{sub} is the Young's modulus of the borosilicate glass, ν_{sub} is the Poisson's ratio of the glass, and h_{sub} is the thickness of the glass. h_{SC} represents the thickness of the SC. Moisturizing treatments affect the development of SC stresses, usually decreasing the peak value. These changes can be used to predict the impact of a treatment on consumer perception [8]. First, a fully hydrated SC was dried in the low-humidity chamber and stresses were measured over the next 20-40 hours. The SC sample was then rehumidified before applying 2 mg/cm² of moisturizing treatment, followed by once again drying the sample in the chamber to measure the developing film stresses. Variations in peak stress are used to quantify the effectiveness of the various moisturizers.

Synchrotron X-Ray Diffraction Measurements

Small-angle X-ray scattering (SAXS) and wide-angle X-ray scattering (WAXS) experiments were conducted at Beamline 11-1 at the Stanford Synchrotron Radiation Lightsource (SSRL). The incident X-ray energy was set to 15 keV, calibrated using the Pb L₃ absorption edge. The beam was focused at the SAXS detector and the calculated photon flux at the sample position was approximately 3.46×10^9 photons/s.

Scattered X-rays were collected using a Pilatus 1M detector for SAXS at a sample-to-detector distance of 2830 mm, and a Pilatus 100k detector for WAXS. SC samples were mounted on silicon wafers in a humidity-controlled chamber, and time-resolved scans were acquired every 2 minutes. The data was processed using Igor Pro with the Nika package for image reduction and azimuthal integration. Peak fitting for the SAXS intensity profiles of each profile was performed. A power-law baseline was modeled and then subtracted, followed by sequentially fitting pseudo-Voigt peaks within three Q-range segments. Peak positions are constrained harmonically based on known structural relationships, and parameters such as amplitude, FWHM, and position are extracted using non-linear least squares optimization. Two sets of experiments were conducted, each on 1cm² pieces of SC mounted on silicon substrates. *Set 1 Control Experiment:* Male and female SC samples were pre-hydrated for 2 hours at ~100% RH, then scanned for 8 hours during drying in a low RH environment. *Set 2:* Samples were soaked in 3:1 cleanser solutions for 2 hours, then rinsed 3x for 30 seconds each time, then placed on the beamline and were scanned for 8 hours during drying in the low RH enviornment.

Attenuated Total Reflectance Fourier Transform Infrared Spectroscopy (FTIR-ATR)

FTIR spectra were collected using a Nicolet iS50 FT/IR Spectrometer (Thermo Scientific) equipped with an ATR accessory. Two sets of experiments were run. *Set 1:* Fully hydrated pieces of SC were placed on top of the ATR crystal to dry overtime in ambient conditions, and time reolved data was collected. Full contact between the tissue and crystal was assured by placing a polycarbonate beam (PCB) on the surface of the SC. By using the Fieldson and Barbari model, the peak intensity is related to water concentration using the Beer-Lambert law.

In this way, water diffusivity, D [cm²/s], is related to absorbance at any given time, A_t [unitless], using:

$$\ln\left(\frac{A_t}{A_\infty}\right) = \ln\left(\frac{4}{\pi}\right) - \frac{D\pi^2}{4L^2} t$$

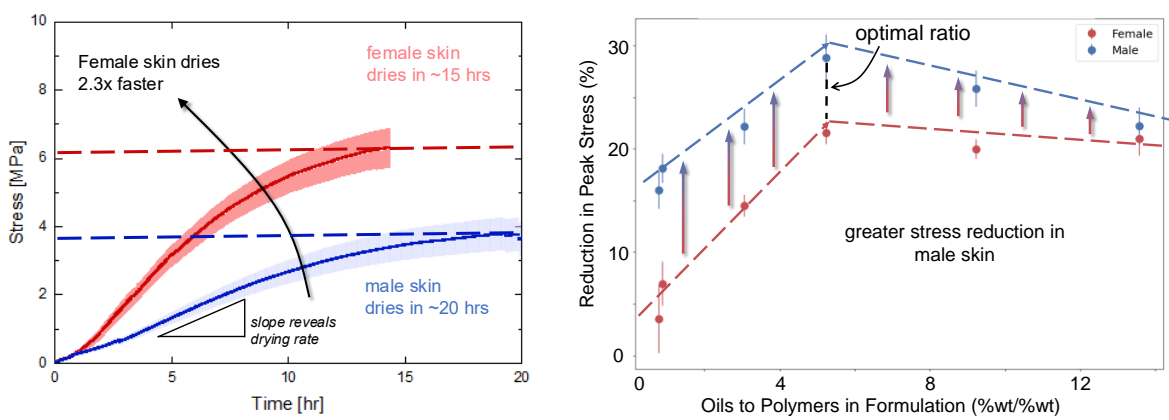
where A_∞ is the asymptotic absorbance value as the SC equilibrates with its environment, t [s] is the time, and L [cm] is the distance from the crystal detector to the edge of the SC.

Set 2: Male and female SC samples were kept in a low RH chamber and then transferred onto the ATR crystal and scanned on the surface for sebum content in 3 different locations on each sample. For each set of experiments, spectra was acquired in ATR mode, in a frequency range of 4,000-525 cm⁻¹, with a resolution of 2 cm⁻¹, a data spacing of 0.241 cm⁻¹, and 16 scans averaged per sample, then was corrected using a linear baseline.

3. Results

Biomechanical Characterization of Male vs. Female Skin

Control drying stress curves, before application of any moisturizer, showed significant differences between male and female skin. Specifically, female skin dried out 2.3x faster than male skin reaching a peak of ~6 MPa in ~15 hours; male skin reached a peak of ~4 MPa in ~20 hours (Fig. 2A). Female SC thickness was slightly smaller than male samples, but not significantly. This indicates that slower water kinetics could likely be due to increased sebaceous gland activity in males, producing a thicker sebum layer that slows water diffusion out of the SC. This could be linked also to a different intercellular lipids organization.



A)

B)

Figure 2: A) Comparison of female (red) and male (blue) control drying curves before application of any formulations. Note that the drying slope of female stratum corneum is larger than male, indicating that female SC dries out ~2.3x faster than male SC. Four female samples and three male samples were averaged, with the bands indicating the standard error. B) The beneficial drying stress reduction was found to be greater in male than female SC for a range of formulations evaluated.

A range of formulations with varying oil to polymer contents were evaluated and in all cases the beneficial reduction in the peak plateau SC stress was found to be greater in male compared to female SC (Fig. 2B).

FTIR-ATR

Analysis of our SC samples revealed that male skin contains approximately twice as much sebum as female skin, confirming higher sebaceous gland activity. This thicker sebum layer likely contributes to slower surface water evaporation, which may explain the delayed buildup of drying stress observed in male samples. To further understand SC water kinetics, we conducted dehydration experiments using FTIR-ATR similar to those used for drying stress measurements. From these, we calculated the lateral diffusion coefficient of water within the SC (Fig 3). In female skin, this coefficient was approximately $8.63 \times 10^{-7} \text{ cm}^2/\text{s}$, while in male

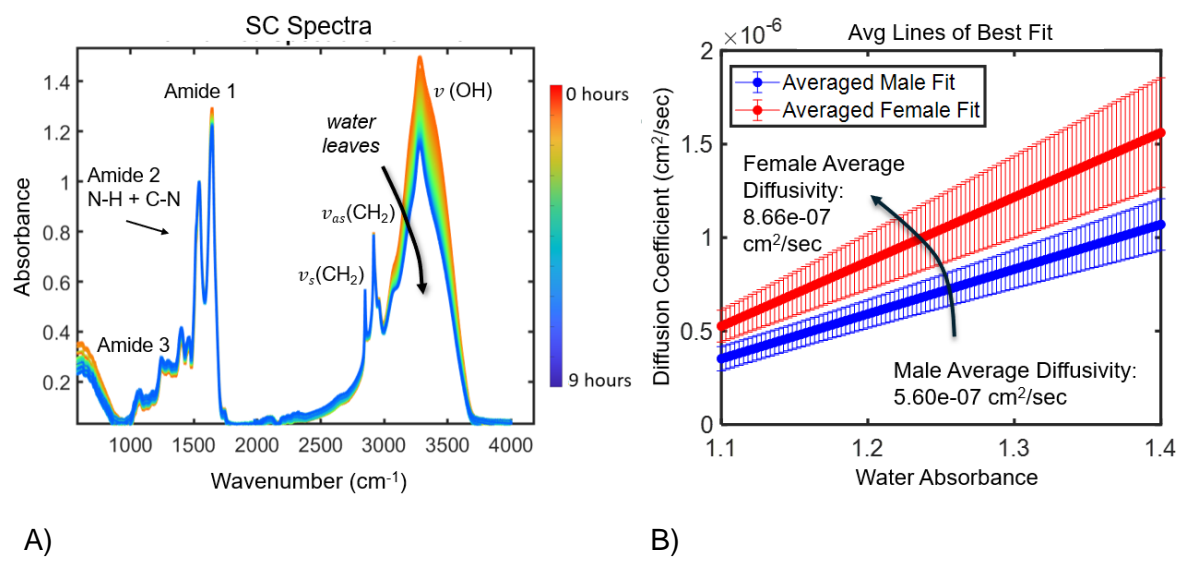


Figure 3. A) FTIR-ATR spectra from female SC drying out on the ATR crystal for 9 hours, specifically tracking the $\nu(\text{OH})$ Peak Intensity. B) Calculated diffusion coefficients (with standard error bands) over time for male and female SC at the same water concentrations.

skin it was lower at $5.60 \times 10^{-7} \text{ cm}^2/\text{s}$. Since lateral diffusion reflects movement through the SC's internal structure, not across the surface, these results point to sex-based differences in SC microstructure

XRD and SAXS

Differences in lipid organization (e.g., LPP and SPP spacing) and corneocyte morphology likely contribute to slower water mobility in male skin. These structural features would also influence the previously seen peak mechanical stress during drying.

XRD spectra have revealed the internal lipid lamellar structure of the stratum corneum (SC). These measurements indicate that male skin exhibits a smaller crystalline spacing between lipid lamellae, which could contribute to its slower rate of water loss. Specifically, the long-periodicity phase (LPP) displays a repeat distance of 12.6 nm, corresponding to a first-order diffraction peak at approximately $q \sim 0.50 \text{ nm}^{-1}$, with second- and third-order peaks at q

$= 1.00 \text{ nm}^{-1}$ and $q = 1.00 \text{ nm}^{-1}$, respectively. While the first two orders are often occluded by overlapping signals, the third-order LPP peak has consistently shown tighter packing in male SC (12.12 nm) compared to female SC (12.60 nm).

Using high-resolution synchrotron XRD and thorough peak fitting analysis (Fig. 4A), we are able to resolve the LPP and SPP peaks across a drying time course (Fig. 4B), capturing data from fully hydrated to dry states. Based on initial analysis and previous results, we hypothesize that male SC will exhibit consistently closer LPP and SPP spacing across all hydration levels. Given that the SPP is more sensitive to water-induced swelling and structural disorder, we also anticipate larger shifts in SPP spacing and amplitude in female SC, whereas SPP in male SC

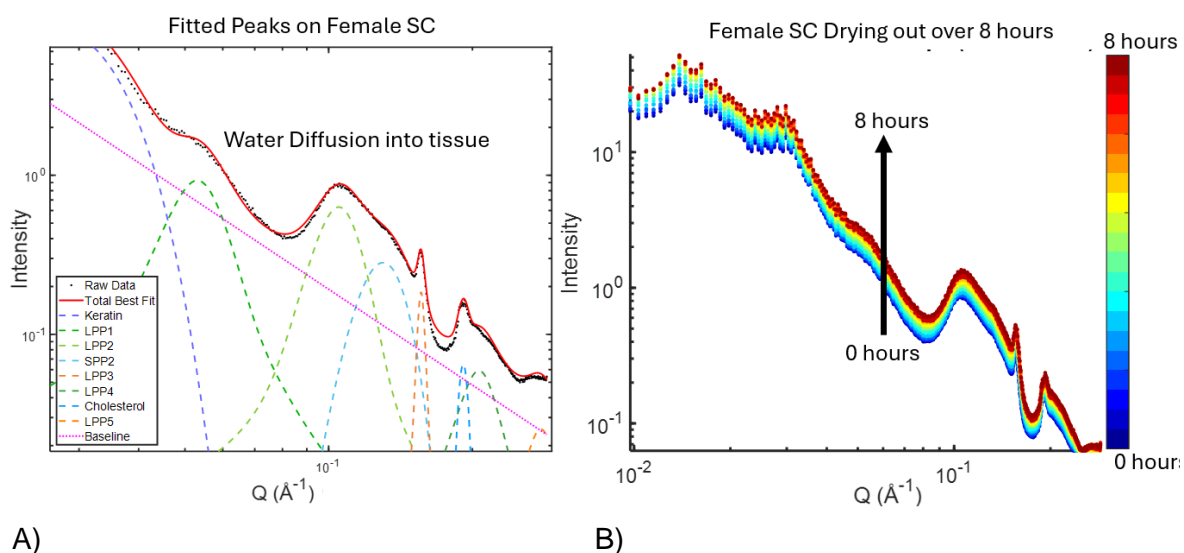


Figure 4. A) Synchrotron XRD spectrum from female SC, with fitted peaks corresponding to keratin, LPP1–LPP5 (long-periodicity phase), cholesterol, and SPP2 (short-periodicity phase). B) Time-resolved XRD scans collected every 25 minutes on the same sample, capturing structural changes in the SC during progressive drying.

may remain more stable. Additionally, we may observe a direct link between tighter lipid packing and reduced keratin swelling in male SC. If true, this could suggest that male SC requires stronger penetration enhancers to achieve effective hydration or delivery of actives, while female SC, despite being more permeable, may benefit from gentler moisturizers and cleansers to avoid barrier disruption.

Neurological Modeling

Neurological modeling for both male and female skin revealed similar trends in the predicted firing rates with ex vivo skin samples and treatments (Fig. 5). In other words, treatments that caused greater stress reductions resulted in lower predicted neural activation that is associated with improved skin comfort. However, male study participants did not report the same level of lower perceived levels of tightness compared to female reports. Female participants demonstrated a closer correlation between predicted neural activity and reported skin tightness observed in our previous studies that relate sensory neuron activation from topical treatments and demonstrate that it modulates the sensorial perception of skin [9]. These findings suggest

that male skin may be less neurologically responsive to mechanical changes related to dry skin or that males are less likely to either perceive or report skin sensorial perception. This striking difference highlights the need to account for sex-specific sensory perception when evaluating product efficacy and the sensory feel on consumers' skin.

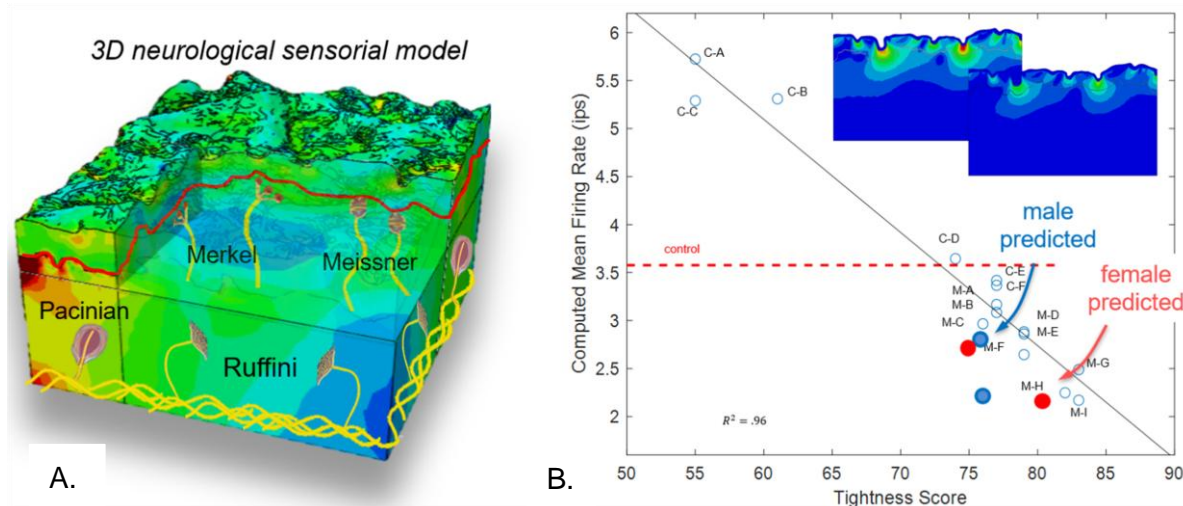


Figure 5. A) 3D neurological model of cutaneous mechanoreceptors involved in sensing skin tightness. B) Graph of the computed mean firing rate of the electrical activity of the mechanoreceptors in the SC vs the consumer percieved tightness score.

4. Discussion

In this study, we show fundamental differences that exist in the biomechanical and barrier properties of male and female stratum corneum. We link these differences to specific structural and compositional distinctions seen between the two tissues, and how these structural differences play a role in the consumer sensory experience following cosmetic treatments.

We conclude that male skin has more sebum on its surface, indicated by FTIR-ATR. This sebum layer helps slow down water loss from the SC and helps explain why stress development occurs less rapidly in the sebum-rich male SC than in the female one. We also saw slower water loss rates in FTIR-ATR where the water difused out from the SC laterally. This points to another structural reason why male skin has slower water kinetics. Investigation with XRD showed that there is tighter packing of lipid lamellar structures such s the LPP and SPP in male tissue which may also help contribute for this decrease in stress rate. These are not generalatized statements due to the small sample size that we have experimented on thus far. Skin barrier properties heavily depend on body location, race, environment, dermatoses, and social behaviors. Therefore, when formulating cosmetic moisturizers for individual consumers, rather than sex or gender, a better metric to use is sebum causal levels.

We investigated several moisturizing treatments *ex vivo* to evaluate their efficacy in male versus female stratum corneum (SC). Stress reduction was consistently greater in male SC, indicating higher moisturizer efficacy, likely due to enhanced water retention in the tissue.

However, when neurological modeling was applied, male-reported skin comfort exhibited surprising insensitivity compared to female reports, even though the moisturizers were objectively more effective on male skin. We note parenthetically that neurological modeling on male and female skin with different skin layer parameters (thickness and stiffness as noted in Fig. 1) did not suggest significant differences in neural activation in a sensitivity analysis. However, the decreased dehydration in male SC did provide significant differences and our future studies are directed to fully developing our male modeling capability to the same fidelity as the current female model.

Two possible explanations for the increased moisturizer efficacy in males are proposed: first, the presence of a thicker sebum layer may help retain hydration following formulation application, although the precise mechanisms remain unclear. Further experimentation, such as selectively removing the sebum layer from male SC, is needed to fully understand this process. Nonetheless, the collected data allow us to predict how a consumer may respond to a given moisturizer and how it will influence their perception of skin feel. In this way, we corroborate our previously established relationship between drying stress reduction and consumer perception scores, and emphasize the importance of tailoring cosmetic treatments to account for sex-specific skin differences.

5. Conclusion

Key findings revealed significant sex-based variations in skin physiology. Male skin displayed slower drying stress development, suggesting slower water loss kinetics. Female SC, conversely, exhibited approximately 50% higher dehydration rates and reached stresses up to 70% greater post-dehydration compared to male counterparts. Male SC also demonstrated increased thickness, enhanced hydrophobicity, a more ordered and closely packed arrangement of intercellular lipids, and significantly higher sebum levels. Interestingly, all moisturizing formulations tested showed greater efficacy on male SC, resulting in improved hydration and an average 48% decrease in dehydration-related stress, a factor correlated with perceptions of skin tightness. Formulations higher in polymer/silicone content increased stress, while those richer in oils/polyols demonstrated a stress-reducing effect, with an optimal ratio.

Neurological modeling yielded an unexpected finding: male-reported skin comfort exhibited surprising insensitivity compared to female reports. These findings reveal critical biological and sensory differences between male and female skin, emphasizing the need for sex-specific considerations in cosmetic formulation. Together, they establish a framework for designing and evaluating personalized skincare treatments at a scale far beyond the limitations of traditional clinical trials.

Conflict of Interest Statement.

HLB, ML, AB, GSL, and AP are employees of L'Oréal Research and Innovation, Aulnay-sous-Bois, France and Chevilly-Larue, France.

SHR, AD, RPR, and RHD have received funding from L'Oréal to perform this research.

References

- [1] Hendrickx-Rodriguez S, Hubiche A, Humbert P, Clarys B, **2022**, Int J Cosmet Sci, **44**, 486–499, <https://doi.org/10.1111/ics.12797>
- [2] Jacobi U, Gautier J, Sterry W, Lademann J, **2005**, Dermatology, **211**, 312–317, <https://doi.org/10.1159/000088499>
- [3] Luebberding S, Krueger N, Kerscher M, **2013**, Int J Cosmet Sci, **35**, 477–483, <https://doi.org/10.1111/ics.12068>
- [4] Man MQ, Hupe B, Sun S, Elias PM, **2009**, Skin Pharmacol Physiol, **22**, 190–199, <https://doi.org/10.1159/000231524>
- [5] Mizukoshi K, Akamatsu H, **2013**, Skin Res Technol, **19**, 91–99, <https://doi.org/10.1111/srt.12012>
- [6] Levi K, Kwan A, Rhines AS, Gorcea M, Moore DJ, Dauskardt RH, **2010**, Br J Dermatol, **163**, 695–703, <https://doi.org/10.1111/j.1365-2133.2010.09937.x>
- [7] Levi K, Weber RJ, Do JQ, Dauskardt RH, **2010**, Int J Cosmet Sci, **32**, 276–293, <https://doi.org/10.1111/j.1468-2494.2009.00557.x>
- [8] Berkey C, Biniek K, Dauskardt RH, **2021**, Extreme Mech Lett, **46**, 101327, <https://doi.org/10.1016/j.eml.2021.101327>
- [9] Bennett-Kennett R, Pace J, Lynch B, Domanov Y, Luengo GS, Potter A, and Dauskardt RH, PNAS Nexus, 2 [9], 1-12, 2023. <https://doi.org/10.1093/pnasnexus/pgad292>